

## Flow Patterns and Water Wetting in Oil-Water Two Phase Flow – A Flow Loop Study

Kok Eng Kee\*, Sonja Richter, Marijan Babic, Srdjan Nesic

Institute for Corrosion and Multiphase Technology

Ohio University, Athens, OH 45701

\*Universiti Teknologi Petronas, Malaysia

### ABSTRACT

Carbon steel pipelines used for transporting oils generally have some water flowing concurrently with the oil phase. The presence of water can lead to internal corrosion problems when free water contacts/wets the pipe wall surface. Therefore, it is pertinent to study how the distribution of water under different oil-water flow conditions can affect the steel surface wetting, i.e. whether the wall surface is wetted by water or oil phase.

In this experimental work, a large scale 0.1m ID inclinable flow loop was used to study the two phase oil-water flow in horizontal and vertical positions. Paraffinic model oil and 1wt% NaCl aqueous solutions were utilized as the test fluids. Two measurement techniques: flush mounted conductivity pins and high speed camera were employed for surface wetting determination and flow patterns visualization, respectively. The wetting data were classified based on four types of wetting behaviors: stable water wet, unstable water wet, unstable oil wet, and stable oil wet. The wetting results from the conductivity pins were found to match with the visualization results from the high speed camera. The horizontal oil-water flow results showed that water flows separately and wets the pipe bottom at low mixture liquid velocity. Moreover, not all of the water is fully dispersed at higher mixture liquid velocities, as traces of water can still be found to wet the surface intermittently.

**Key words:** water wetting, oil-water flow, flow pattern, conductivity pin, wettability, corrosion

### INTRODUCTION

In the oil industry, formation water is often produced along with the crude oil and transported in carbon steel pipelines. Some of the primary parameters in internal corrosion assessment of pipelines are the presence of free water and the content of corrosive species such as CO<sub>2</sub>, H<sub>2</sub>S, organic acids etc. Since the corrosive species are soluble in the aqueous phase, the likelihood of internal corrosion increases when the water systematically separates out of the oil stream and comes into contact with the pipe wall surface, a scenario known as “water wetting”. On the other hand, “oil wetting” takes place when the wall surface is wetted by oil phase and the water is entrained. Oil wetting retards the corrosion rate since the corrosive species do not come into direct contact the pipe wall. In an oil-water flow with oil as the dominant phase and water as the dispersed phase, varying degree of dispersion driven by the flow can lead to different flow regimes in the pipe. The water wetting of the internal pipe wall is closely related to how the water is distributed in the oil-water flow, and this affects the occurrence of internal corrosion.

The horizontal oil-water flow patterns can be classified into two broad categories: separated and dispersed flows, according to the distribution of the phases.<sup>1</sup> At a low flow rate, the oil and water flow separately as continuous phases. As the oil flow rate increases, the flow has sufficient energy to entrain and break up the heavier water into droplets. Some relevant oil-dominated flow patterns are described below and illustrated in Figure 1:

*Separated flow:*

- o *Stratified smooth (ST-S)*, continuous oil and water phases separated with a smooth interface.
- o *Stratified with globules (ST-G)*, swarms of closely packed water globules/droplets flowing at the lower half of the pipe.
- o *Stratified with mixing layer (ST-M)*, a dispersion layer at the oil-water interface which includes water-in-oil dispersion and oil-in-water dispersion.

*Dispersed flow:*

- o *Semi-dispersed (S/D)*, where dispersed water droplets are suspended and distributed with an increasing concentration towards the lower half of the pipe.
- o *Fully-dispersed (D)*, where water droplets are distributed evenly across the pipe.

It is noted that perfectly horizontal pipelines seldom exist in the field. Any change in the pipe inclination may affect the phase distribution. For example in an upward inclined pipe, water phase flows slower because of the gravity force pulling the denser phase down an inclined plane, resulting in an increased water holdup. The opposite is true for downward inclined pipe in which the water flows faster.

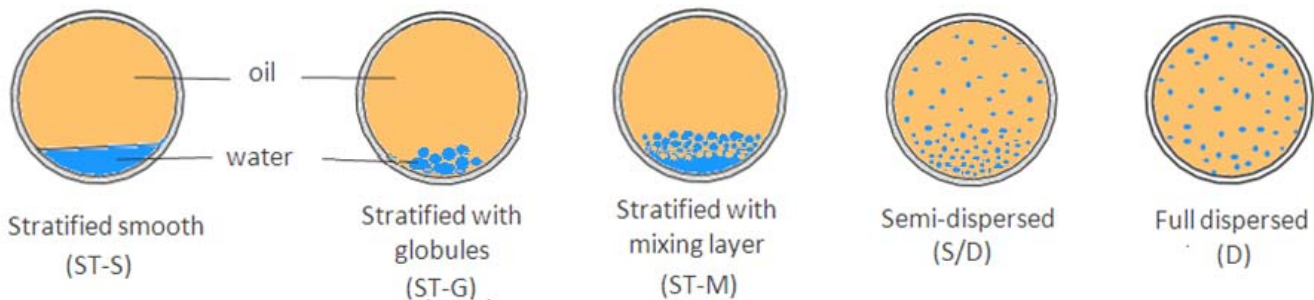


**Figure 1: Schematics of flow patterns in horizontal oil-water flow: separated and dispersed flow patterns**

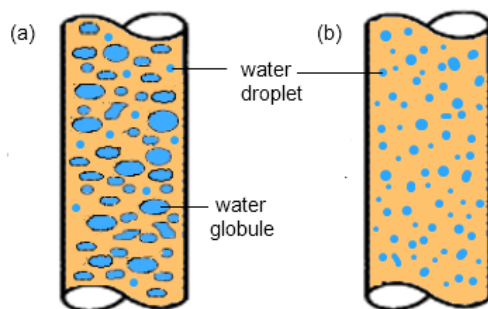


**Figure 2: Schematics of flow patterns in vertical oil-water flow (a) dispersed globules flow pattern, (b) dispersed droplets flow pattern**

While separated flow can be observed in horizontal or near-horizontal pipes, it does not exist in inclined and vertical flow.<sup>2</sup> For the oil-dominated flow conditions two types of dispersed flow patterns can be observed in vertical upward flow. They are *dispersed droplets* and *dispersed globules*, as shown schematically in Figure 2.

- o *Dispersed globules:* seen at low flow rate where the discrete water droplets and larger water globules intermix together in the oil-continuous phase. The droplets are round and the shape is

dominated by surface tension. The larger globules are either have flattened oval or irregularly deformed shape. Sphericity is lost if the drop characteristic size is larger than the capillary length,  $L_c = (\sigma/\Delta\rho g)^{1/2}$ , governed by the surface tension and gravity. One may find  $L_c \sim 5\text{mm}$  for water-oil system, with interfacial tension  $\sigma = 40\text{ mN/m}$ , and density difference is  $\Delta\rho \sim 160\text{ kg/m}^3$ .

- *Dispersed droplets*: occurs at higher flow rate where small round water droplets are dispersed uniformly in oil-continuous phase. The droplets are seen to flow in a relatively straight path almost as fast as the oil phase.

In horizontal oil-water flow, the pipe position at six o'clock (bottom of the line) is the most susceptible to corrosion, where the water can drop out because of its higher density and wet the pipe surface. In vertical oil-water flow, there is no preferential wetting location around the pipe as the gravity does not exert itself toward the pipe wall. There has been a number of large scale flow loop work done on the oil-water flow patterns and their relation with hydrodynamic parameters such as pressure drop and holdup.<sup>2-6</sup> Little or no emphasis was put on water wetting or distribution of the water phase in these studies. Researchers at Ohio University employed electrical conductivity probes installed in a flow loop to study the water wetting in oil-water flow.<sup>1,7-10</sup> In another work, Valle used electrical conductance probes to study the relation of water exposure and corrosion.<sup>11</sup> Angeli and Hewitt employed a high frequency impedance probe to determine the local phase fraction and a single conductivity pin to identify the continuous phase in dispersed flow.<sup>12</sup>

The present work focused on studying the flow patterns as well as the corresponding water wetting behavior in a large scale flow loop. The oil is used as the continuous phase and the water as the secondary phase with water cut up to 20%, as can be commonly found in oil production field conditions.

## EXPERIMENTAL

The experiments were conducted in a large-scale inclinable multiphase flow loop used for the study of gas-liquid, liquid-liquid, and gas-liquid-liquid flow system. The main part of the flow loop consists of a 150 ft (45 m) long, 4-in (10.2 cm) ID flow line mounted on a steel rig structure. This section of the loop is fully inclinable from 0° (horizontal) to a 90° (vertical). Oil and water liquids are pumped separately from the storage tank into the main flow line by progressive cavity pumps. The oil flow is connected to the main line while the water flow is directed to the main line via a T-section. The fluid mixture flows for approximately 100 pipe diameters to attain a fully developed flow pattern before entering the upstream test section made of carbon steel, used for surface wetting measurement, followed by a transparent PVC section, used for flow pattern visualization. A picture of the upstream test section is shown in Figure 3. Once leaving the flow loop, the immiscible fluids are separated in a liquid-liquid separator and returned to the respective storage tank before being re-circulating into the flow loop. The oil phase used in the present experiments was a refined paraffinic oil, commercial trade name: LVT 200\* and a water phase used was 1%wt. NaCl solution prepared from de-ionized water and analytical grade reagent. The schematic layout of the closed-loop system is shown in Figure 4.

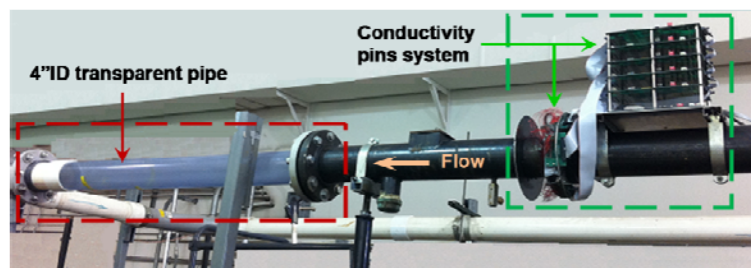


**Figure 3: The 4" ID transparent pipe and pin test section fitted with conductivity pins.**

\* Trade name

©2014 by NACE International.

Requests for permission to publish this manuscript in any form, in part or in whole, must be in writing to NACE International, Publications Division, 1440 South Creek Drive, Houston, Texas 77084.

The material presented and the views expressed in this paper are solely those of the author(s) and are not necessarily endorsed by the Association.

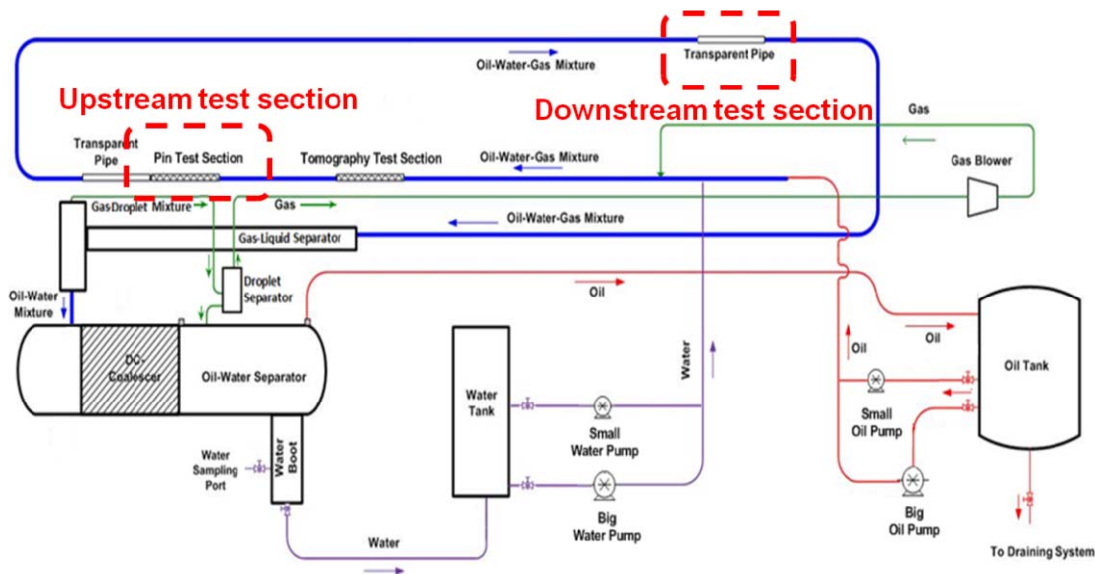


Figure 4: Schematic layout of the inclinable 4" ID flow loop used for oil-water flow. 1

## High Speed Camera

The high speed camera used was Phantom V12.1<sup>†</sup>. It is built with a 1280 x 800 CMOS sensor, capable of 6,000 frames/second (fps) at full resolution. The set up used in the current research included a frame rate of 6,000 fps and exposure of 90-120  $\mu$ s to record the flow patterns through the 4" ID transparent PVC pipe. The transparent pipe was illuminated with a bright white light source (2.4 kW) with a light diffuser in between. The light source was positioned behind the transparent pipe such that the illumination through the pipe would be directly opposite the camera lens on the other side of pipe

## Conductivity Pins

The conductivity pins are flush mounted in a mild steel test section covering the lower half (180°) of the pipe as shown in Figure 5, named as 180° pins section. The pins are sequentially activated by applying a square wave oscillating voltage from 0V to +4.5V at 100 Hz. If the pin surface is covered by water, the fluid resistance is low, and vice versa for the pin covered by the oil phase. The wetting information for all the pins is displayed simultaneously as a pictorial wetting snapshot shown in Figure 5(b).

In this work, the array of pins flush mounted on the pipe wall served as the most important sensor that can detect the interaction between the fluids and the pipe surface. The current pin design is an upgraded version of a pin array design, used in previous work.<sup>1</sup> The current pin system is more robust and more sensitive in detecting the presence of a water film or droplets in contact with the pin. The original design was of made using 20 AWG (American Wire Gauge) 0.032" OD stainless steel (SS) pin insulated with epoxy flush mounted in a 1.6 mm (1/16") hole with the conductivity measured between the pin and the surrounding pipe wall. The original design was suffering from galvanic corrosion in the vicinity of the pins leading to degrading performance. The upgraded design consists of the same 20 AWG SS pins which are encased with epoxy in a 1.5 mm (0.06") SS sleeve. The pin assembly is then insulated with epoxy and flush mounted in a 1.6 mm hole. The new design pin is more sensitive and robust since the conductivity being measured is between the pin and the sleeve which are of the same SS material and not prone to corrosion. Before running each test, it was important to perform a thorough test section polishing followed by half-hour continuous "rinse" with gas-oil flow (using a clean model oil) to remove any grime/impurities/dirt that may have deposit on the pins.

<sup>†</sup> Trade Name

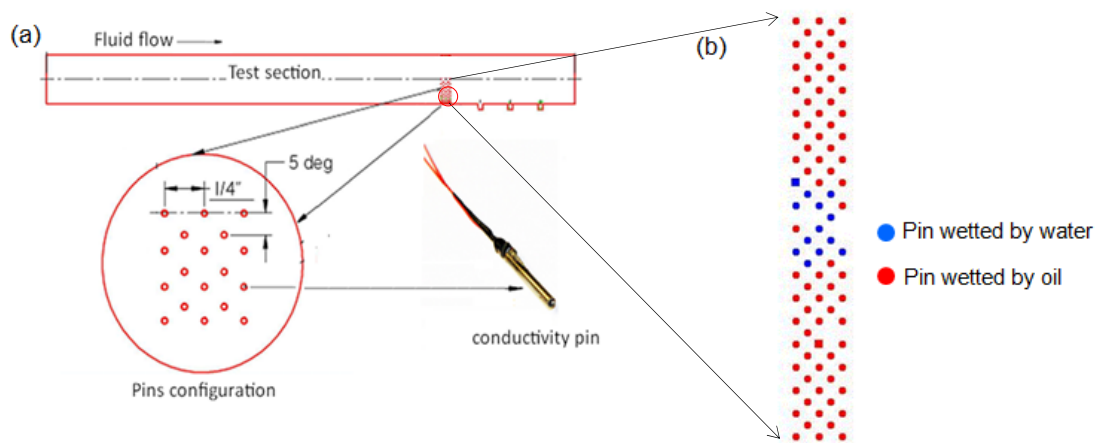


**Figure 5: a) Schematic conductivity pin array layout flushed mounted on the lower half of the pipe wall covering lower 180°, (b) Typical conductivity pins array snapshot.**

## Test Matrix

The flow loop was setup to study the oil-dominated flow in both horizontal and vertical pipe configuration with water cuts up to 20%. A total of 111 flow regimes have been recorded for the various test conditions as shown in Table 1.

The experimental sequence was executed by increasing water cut at a given fixed mixture liquid velocity. The mixture liquid velocity is the sum of superficial oil and superficial water velocities. Wetting points were measured after the flow was fully developed and consistent wetting behavior was achieved.

**Table 1**  
**Test matrix for horizontal and vertical oil-water flow.**

System conditions	1 atm. @ 22 °C	
Oil phase	LVT200	
Water phase	1 %wt NaCl aqueous solution	
Pipe ID (in)	4	4
Inclination (°)	0	90
Mixture Liquid Velocity (m/s)	0.2 – 1.7	0.5 – 1.5
Water cut %	1 - 20	1 - 20
Test points	70	41

## RESULTS AND DISCUSSIONS

### Horizontal Flow Patterns

Sample images of some horizontal flow patterns obtained from the high speed camera are presented in Figure 6. The flow pattern recorded at mixture liquid velocities from 0.2 to 1.5 m/s are compared at varying water cuts from 5 to 20%. At mixture liquid velocities less than 1.5 m/s, various forms of separated flow patterns were observed for all tested water cuts. *Stratified smooth* (ST-S) flow patterns were observed at the lowest mixture liquid velocity (0.2 m/s), where the oil-water interface is undisturbed due to low level turbulence in the flow. *Stratified-globules* (ST-G) flow patterns were seen at the slightly higher mixture liquid velocities when the turbulence in the flow managed to break up the relatively small amount of water into a swarm of closely packed droplets/globules that flowed in the pipe

bottom. At higher water cut (20%), *stratified with mixing layer* (ST-M) flow patterns were observed in which the water flowed as a continuous layer at the pipe bottom with a dispersion layer at the oil-water interface. *Semi-dispersed* (S/D) flow patterns were observed at the mixture liquid velocity of around 1.5 m/s. At the mixture velocity  $\geq 1.5$  m/s, *dispersed* flow pattern was seen at lowest water cut of 1% where water droplets were entrained and suspended more-or-less evenly across the pipe cross section. With increasing water cut, the flow pattern changed to *semi-dispersed* where water droplets were found to concentrate more in the lower half of the pipe. Figure 7 shows the flow pattern map for horizontal oil-water flow. Empirical transition lines (dashed lines), delineating each flow pattern in horizontal oil-water flow, are included in the map.

By analyzing the high resolution video files, various flow characteristics can be extracted including the water droplet size. In pipe flow, the breakup of droplet occurs when the surface tension force holding a droplet together is exceeded by the local fluid inertial force generated by the turbulent fluctuations as described by Hinze.<sup>13</sup> The higher the turbulent energy of the flow, the smaller the droplet size dispersed in the flow. The water droplet size is Figure 8 shows the images of dispersed water droplets for water cuts from 5% to 20% at mixture liquid velocities of 0.5m/s and 1m/s. From the images, the droplets were observed to generally increase in size with increasing water cut from 5% to 10% at fixed mixture liquid velocity. This would correspond to lower turbulent force exerted by the continuous oil phase needed to break up the water. Besides there is a high probability of water droplets coalescing into larger ones at high water cut. It was observed that the water droplets generally decreased in size with increasing mixture liquid velocity from 0.5m/s to 1m/s at a fixed water cut. This was attributed to an increase in turbulent energy which could break up and disperse the water into smaller droplets.

The maximum droplet size,  $d_{max}$  was determined by measuring the chord lengths of the largest spherical drops observed in the flow field according to the images obtained with the high speed camera.  $d_{max}$  values were then averaged from 20 frames for each experimental condition. The results are plotted in Figure 9 which depicts the measured droplet size with varying mixture liquid velocity at fixed 1% and 5% water cuts. The maximum size of water droplet is observed to reduce with increasing mixture liquid velocity from 0.5 to 1.7m/s, with overall reduction of 50%. However, the change of water cut from 1% to 5% has minimal effect on water droplet size. The difference between the measured values for the two cases is within the range of uncertainty of measurement.

The measured  $d_{max}$  values were then compared with the calculated values from the Water Wetting Model using equation (1).<sup>14</sup> This model is used to predict the transition between settling and entrainment of droplets and by extension distinguished between oil and water wetting.

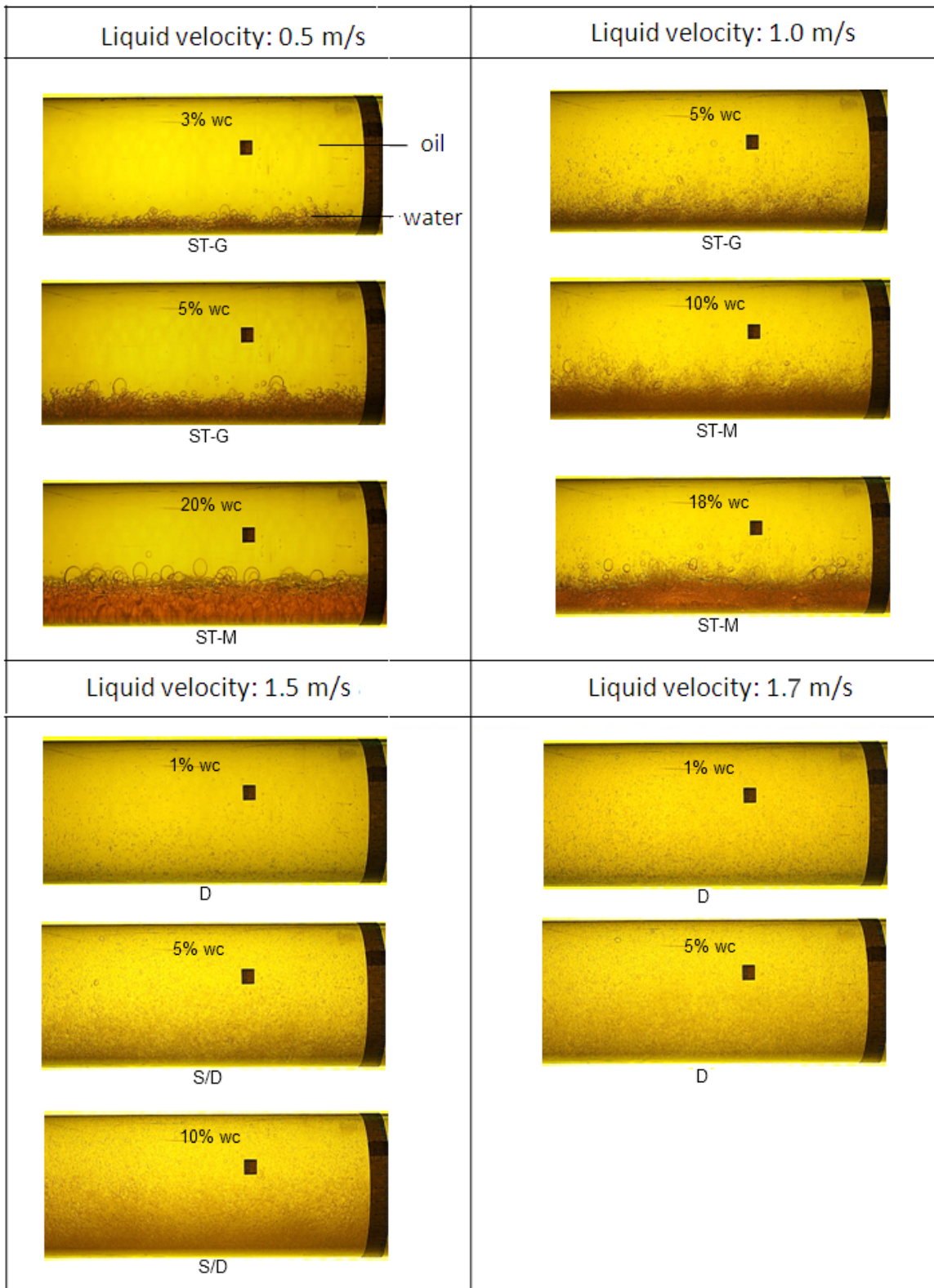
$$\left( \frac{d_{max}}{D} 2U_{so}^3 f \frac{\rho_m}{\rho_o (1 - \varepsilon_w)} \right)^{2/3} = \frac{\varepsilon_w \sigma}{\rho_o (1 - \varepsilon_w)} \left( C_H \left( \frac{6}{d_{max}} - \frac{4 \sin \alpha}{\varepsilon_w \pi D} \right) + C_W \frac{4 \alpha \cos \theta}{\varepsilon_w \pi D} \right) \quad (1)$$

$D$  is the pipe diameter,  $\rho_o$  is the oil density,  $\rho_m$  is the mixture liquid density,  $\varepsilon_w$  is the water cut,  $\sigma$  is the oil-water interfacial tension,  $U_{so}$  is the superficial oil velocity,  $f$  is the friction factor,  $\alpha$  is the water wetting angle,  $C_H$  and  $C_W$  are the empirical factors,  $\theta$  is the oil-in-water contact angle on the steel surface.

In Figure 9, both the measured and the predicted values are plotted for water cuts of 1% and 5%. The transition from stratified to dispersed flow is predicted by the model when the turbulent energy of the continuous phase is intense enough to break up the dispersed phase into droplets smaller than a critical size,  $d_{crit}$  calculated from equation (2).<sup>14-16</sup>

$$d_{crit} = \text{Min} \left( d_{cg} = \frac{3}{8} \frac{\rho_o U_{so}^2 f}{|\rho_w - \rho_o| g \cos \theta} , d_{c\sigma} = \sqrt{\frac{4\sigma}{|\rho_w - \rho_o| g \cos \theta'}} \right) \quad (2)$$

where  $\rho_w$  is the water density,  $d_{cg}$  is the critical size due to buoyancy,  $d_{c\sigma}$  is the critical size due to deformation of a spherical droplet.



ST-G : stratified with globules  
 ST-M : stratified with mixing layer

S/D : semi-dispersed  
 D : dispersed

**Figure 6: Images of horizontal oil-water flow patterns taken by high speed camera for liquid velocities from 0.5 to 1.7 m/s and water cuts from 5 to 20%.**

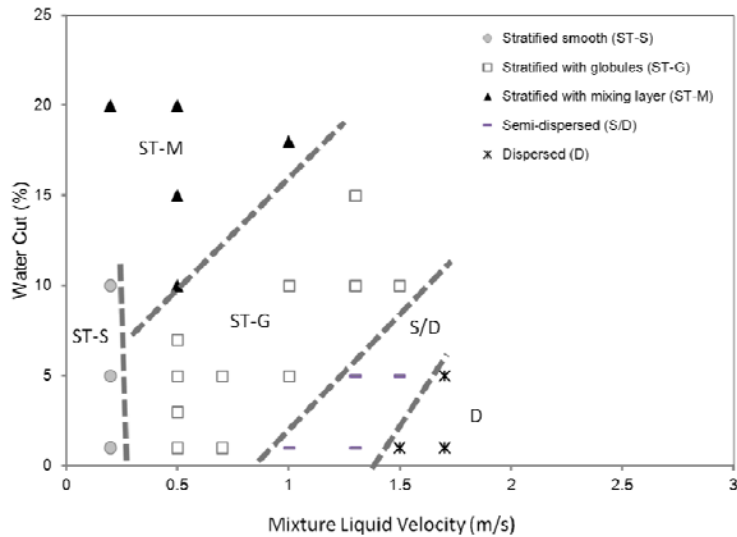


**Figure 7: Flow pattern map for horizontal oil-water flow in 4" ID pipe.**

The intersection point of the two lines created by the model (denoted by a red square in Figure 9) showing calculated  $d_{max}$  and  $d_{crit}$  represents the transition point from stratified flow (to the left of the transition point where  $d_{max} \geq d_{crit}$ ) to dispersed flow (to the right of the transition point where  $d_{max} < d_{crit}$ ). In Figure 9 (a), the predicted transition point at 1% water cut is around 1.2 m/s, and compared quite well with the observed transition from the flow loop at 1.3 m/s. The predicted  $d_{max}$  line matches the general downward trend of the measured  $d_{max}$ , considering the inherent uncertainties in the model. In Figure 9(b), the stratified/dispersed flow transition at 5% water cut is predicted at 1.6 m/s while the observed transition point from the flow loop is around 1.7 m/s. The model seems to compare well with the measured  $d_{max}$  around the transition point, but consistently over predicts at lower velocity range. It is noted that the maximum droplet size was not performed on the tested water cuts larger than 5% since the flow was dominantly in a stratified flow pattern.

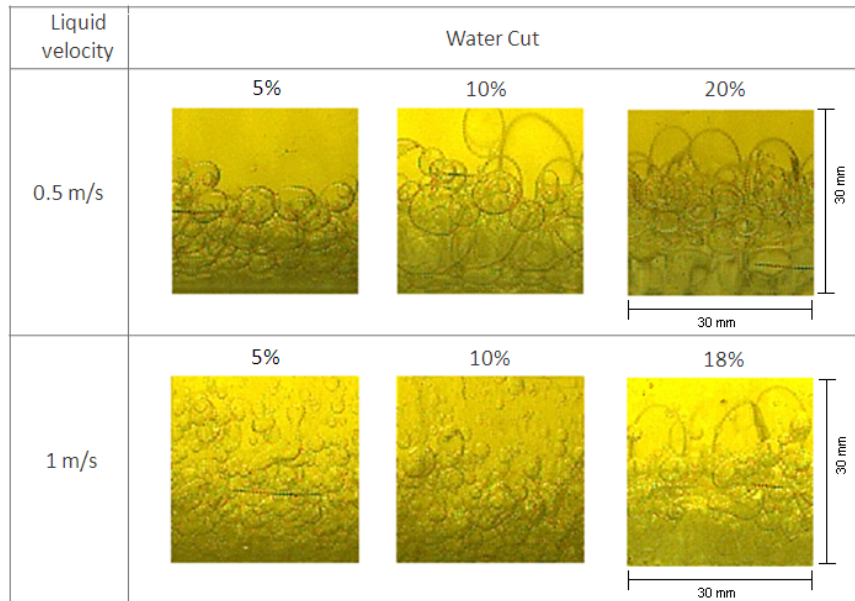


**Figure 8: Images of water-in-oil droplets at mixture liquid velocities of 0.5m/s and 1 m/s with water cuts varying from 5% to 20% in horizontal oil-water flow.**



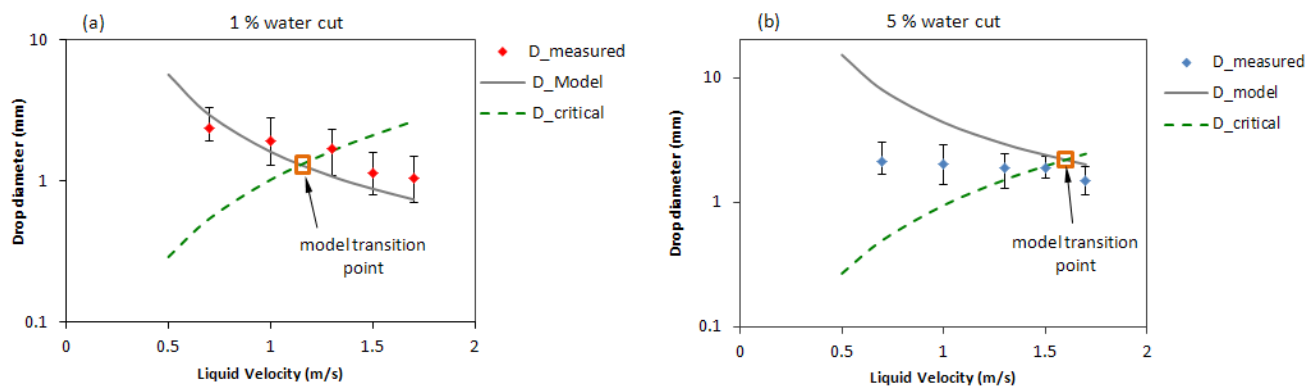


**Figure 9: Experimental droplet size compared with predicted maximum droplet size and predicted critical droplet size for (a) 1% water cut, (b) 5% water cut.**

## Phase Wetting

By analyzing the wetting behavior obtained from the conductivity pins at various flow conditions, four categories of phase wetting regimes were identified:

- Water wetting* : A number of pins are steadily water wet.
- Unstable water wetting* : A number of the pins are water wet, some of those alternate intermittently between oil and water wet.
- Unstable oil wetting* : Only a few of the pins are water wet, some of those alternate intermittently between oil and water wet.
- Oil wetting* : All pins are oil wet.

It is worth noting that both *unstable oil wetting* and *unstable water wetting* display intermittent behavior but with different degree of wetting intermittency. In previous work and publications, these two wetting behaviors were collectively termed as *intermittent wetting*.<sup>1</sup> However, it is recognized that a case where most pins are oil wet with few pins showing intermittent wetting is quite different from another case where most pins are water wet with few pins showing intermittent wetting. From the corrosion standpoint, the latter case would have a much higher likelihood of corrosion since the probability of free water wetting the steel surface for extended periods of time is higher.

Using these phase wetting regimes, the wetting behavior in horizontal flow can be plotted in a phase wetting map as shown in Figure 10, where each data point indicates the phase wetting at a given flow condition. The wetting results were cross-correlated with the flow pattern map in Figure 7. In general, the wetting was greatly affected by the change of water cut and velocity. For a separated flow pattern at low velocity, water wetting occurred at the six o'clock position in horizontal flow, as expected. When transitioning to semi-dispersed and dispersed flow patterns at higher velocity, the wetting showed gradual transition from unstable water wetting to unstable oil wetting behavior. Full oil wetting was not observed even for the highest flow velocities at 1% water cut. A predicted wetting transition line, generated by the water wetting model is also included in the wetting map shown in Figure 10. Comparing it with the experimental data, the model agrees reasonably well in the delineation between unstable water wet and unstable oil wet, which establishes the former case as 'water wetting' when corrosion likely to occur and the latter case as 'oil wetting' when corrosion is much less likely to occur.

The current wetting results were compared to previous wetting results using the old conductivity pin system.<sup>1,10</sup> As shown in Figure 11, the previous wetting results displayed much stronger oil wetting

behavior at lower water cuts (< 3% water cut) and high mixture liquid velocity (>1.7m/s) while the present results showed much more pronounced intermittent wetting varying between unstable oil wet and unstable water wet behaviors. This could be attributed to the increased sensitivity of the improved conductivity pin system that could detect water droplets or a thin water layer on the pipe wall.

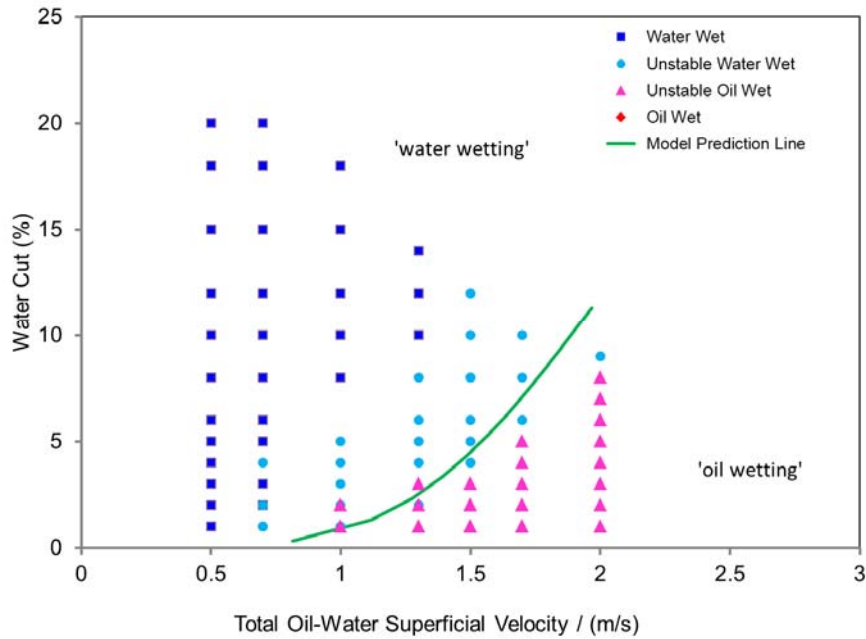


Figure 10: Phase wetting map for horizontal oil-water flow using new pins design.

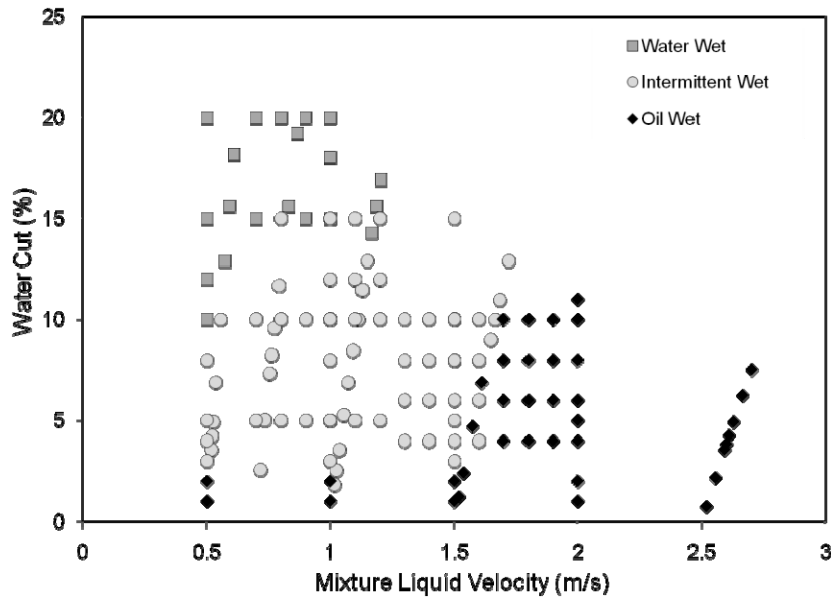
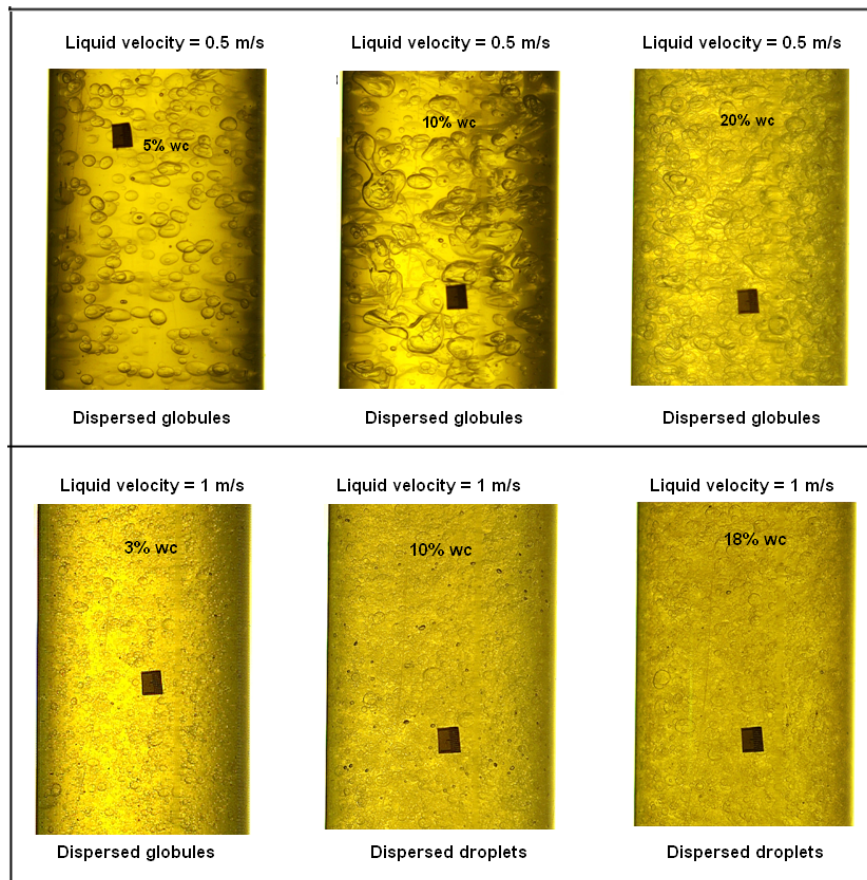


Figure 11: Phase wetting map of horizontal oil-water flow using previous pins design.1

## Vertical Flow Pattern

The vertical oil-water flow pattern results obtained from the high speed camera are presented in Figure 12. For the given test conditions in oil-dominated flow, two flow patterns were identified. At liquid velocity of 0.5 m/s, *dispersed globules* flow pattern occurred where discrete water droplets and larger water globules were dispersed in the flow. The droplets were small and spherical, while the globules were larger and had a more flat/oval shape, travelling upwards with some sideways swerving. The water globules were observed to flow much slower than the droplets, showing noticeable slippage with the oil. An increase in the water cut to 10% resulted in growing of water globules forming larger irregular shapes that deformed unsteadily as they flowed upwards. At 20% water cut, these dispersed water globules ceased to grow in size. The droplets that formed were rounded, packed much closely and became harder to observe as individual droplets. It is believed that the interactions of densely packed droplets bounded by the finite pipe diameter restricted the droplet growth. No water slug/churn was observed at all tested water cuts.

At liquid velocity of 1 m/s, the observed flow patterns showed gradual transition from *dispersed globules* to *dispersed droplets* accompanied by the diminishing occurrence of larger globules. The discrete water droplets were much more sparsely distributed at lower water cut. At higher mixture liquid velocity, the increased turbulence resulted in breakup of water droplets into much finer size that dispersed uniformly across the pipe, which is characterized as the *dispersed droplets* flow pattern. The dispersed droplets were seen to flow upwards with very little slippage with respect to the bulk flow. The flow pattern results for vertical upward oil-water flow are plotted in a flow regime map in Figure 13, showing the flow patterns of *dispersed globules* at lower liquid velocity and *dispersed droplets* at higher liquid velocity. At liquid velocity of 1.5 m/s, the visibility was compromised by the unwanted entrainment of air into the bulk flow from the oil tank, which affected the apparent density/viscosity of the phases.



**Figure 12: Images of vertical oil-water flow patterns at mixture liquid velocities of 0.5 m/s and 1 m/s at varying water cuts up to 20%.**

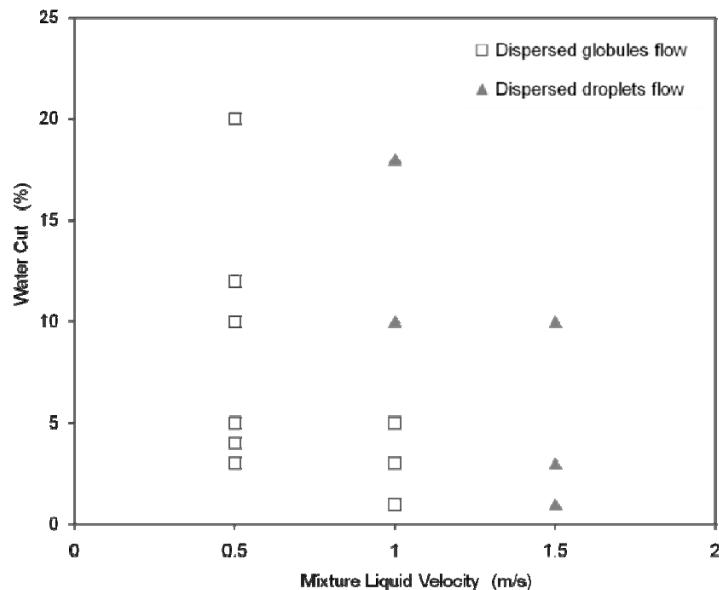


**Figure 13: Flow pattern map for vertical oil-water flow in 4'' ID pipe**

The maximum droplet size  $d_{max}$  was measured by inspecting for the largest spherical droplets in the high speed video recordings. Figure 14 shows the images of dispersed water droplets from 3% to 20% water cut at mixture liquid velocities of 0.5 and 1.0 m/s. The measured  $d_{max}$  values (averaged from 20 droplets) were then compared with the calculated values obtained from the water wetting model (equation 1) and plotted in Figure 15. It can be observed that the measured  $d_{max}$  values increased with water cut until it reached a maximum at 10% water cut. At higher water cut, the interactions of densely packed droplets bounded by the finite pipe diameter could have restricted further droplet growth. At mixture liquid velocity of 0.5m/s, the model predicted quite well for data up to 10% water cut, however, it overpredicted at 20% water cut. At mixture liquid velocity of 1 m/s, the model predicts fairly well compared with the data at mixture liquid velocity of 0.5 m/s.

## Phase Wetting

The wetting results obtained from the conductivity pins are plotted on a wetting map in Figure 16. Each wetting data point in the map indicates the phase wetting regime at given flow condition based on the wetting regimes defined in section above. The results show that oil wetting generally prevails for vertical oil-water flow. The wetting results showed *oil wet* at low water cut that became *unstable oil wet* at higher water cut except for 1 m/s which remained oil wet. For the case of *unstable oil wetting*, the water wetted locations were found to appear randomly over the 180° pins section. Unlike the wetting behavior in horizontal flow, the change of velocity was not seen to significantly affect the wetting. There is an exemption for the water cuts larger than 15% at mixture liquid velocity of 0.5 m/s in which the wetting becomes *unstable water wetting*.

Upon examining the high speed camera recordings, the oil wetting behavior at low water cut can be explained by the sparse distribution of water droplets that flow in a relatively straight path up the pipe, with very little likelihood of impinging on the wall. The findings from the test conditions showed that the tendency of larger size globules to swerve towards the pipe wall was not as prevalent as previously thought by Cai et al.<sup>1</sup> Increasing the water cut above 15% causes the dispersed droplets to grow larger in size and pack more closely. These densely distributed droplets are more likely to contact and wet the pipe wall when they are flowing in close proximity, resulting in unstable oil wetting.

Two important remarks must be made related to this vertical pipe flow study. Firstly, the prevailing oil wetting was found repeatedly in the beginning of experiments. Once any water adhered and wetted the

steel walls, which are naturally more hydrophilic, the water wetting prevailed and water was not easily displaced by the continuous oil flow alone. Secondly, truly vertical pipes rarely exist in the fields. It was observed if the test loop were slightly inclined off-axis from the vertical plane; the risk of water contacting the wall increased because of gravity pulling the heavier phase toward the wall.

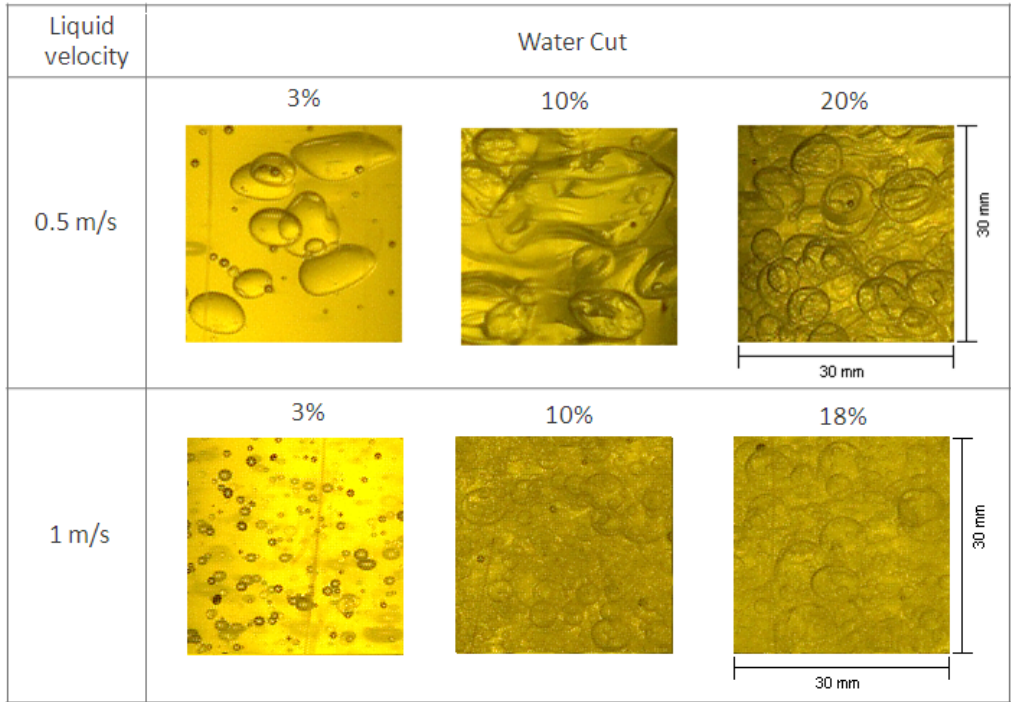


**Figure 14: Images of water-in-oil droplets at mixture liquid velocities of 0.5m/s and 1 m/s at water cuts from 3% to- 10% in vertical pipe flow.**

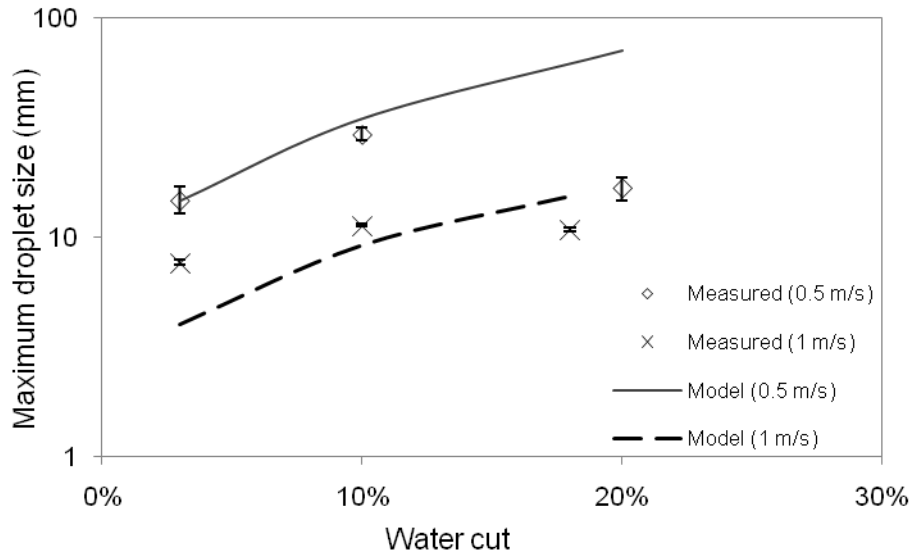


**Figure 15: Comparison of the measured and model predicted maximum droplet size at 0.5 m/s and 1.0 m/s in vertical oil-water flow.**

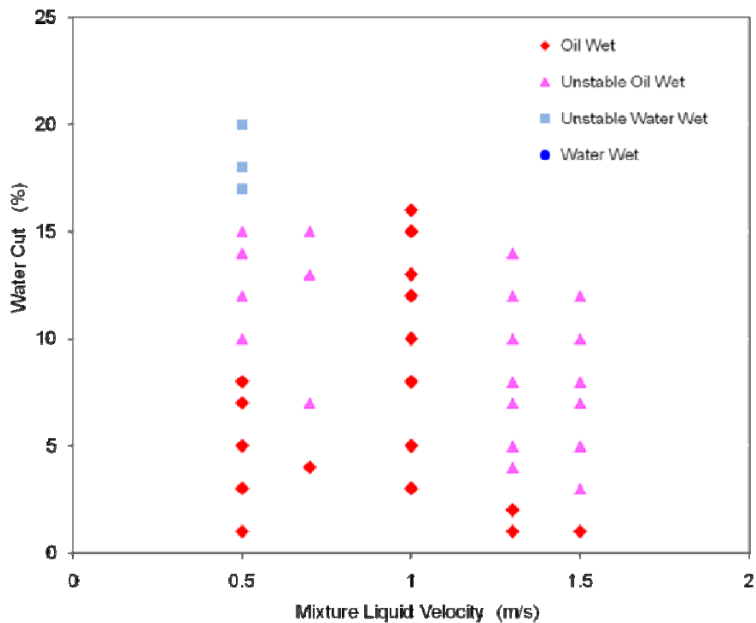


**Figure 16: Phase wetting map for vertical oil-water flow using LVT200 model oil as oil phase and 1 wt% brine as water phase.**

## CONCLUSIONS

1. For the oil-dominated flow experiments, five types of flow patterns were reported in horizontal flow. They are *stratified smooth*, *stratified with globules*, *stratified with mixing layer*, *semi-dispersed* and *dispersed* flow patterns. Two types of flow patterns were reported in vertical flow. They are *dispersed globules* and *dispersed droplets* flow patterns. Separated flow patterns were not observed in vertical flow.
2. In horizontal flow, the pipe bottom was predominantly wetted by the free water layer in separated flow patterns. For semi-dispersed and dispersed flow pattern at higher flow rate, the wetting became unstable oil wetting. No permanent oil wetting was observed in the conditions tested.
3. In vertical flow, the dispersed water droplets/globules were observed to flow upward in a relatively straight path, with a low tendency of swerving. The wetting was predominantly detected to be oil wet across the tested velocity range. The change of velocity was not observed to affect the wetting. For water cuts above 15% at low mixture liquid velocity, unstable water wetting was observed which could be associated with the existence of densely distributed water droplets/globules close to the pipe wall.
4. The maximum droplet sizes was measured in different flow regimes and compared with the water wetting model prediction. They were in reasonable agreement except for the case of 20% water cut in vertical flow.

## ACKNOWLEDGEMENTS

The authors wish to thank the financial support and technical directions from the sponsoring companies: BP, ConocoPhillips, ExxonMobil, Petrobras, Saudi Aramco, and Total. Discussion with Dr. Luciano Paolinelli is greatly appreciated. Support from Universiti Teknologi Petronas is appreciated

## REFERENCES

1. J. Cai, C. Li, X. Tang, F. Ayello, S. Richter, and S. Nestic, "Experimental study of water wetting in oil-water two phase flow-Horizontal flow of model oil," *Chemical Engineering Science*, vol. 73, (2012): pp. 334–344.
2. J. Flores, X. Chen, C. Sarica, and J. Brill, "Characterization of Oil–Water Flow Patterns in Vertical and Deviated Wells," *SPE Production & Facilities*, vol. 14, no. 2, (1999): pp. 102–109.
3. J. Trallero, C. Sarica, and J. Brill, "A study of oil-water flow patterns in horizontal pipes," *SPE Production & Facilities*, vol. 12, no. 3, (1997): pp. 165–172.
4. G. W. Govier, G. A. Sullivan, and R. K. Wood, "Upward vertical flow of oil-water mixtures," *Canadian Journal of Chemical Engineering*, vol. 39, no. 2, (1961): pp. 67–75.
5. H. Shi, J. Cai, and W. P. Jepson, "Oil-water two-phase flows in large-diameter pipelines," *Journal of Energy Resources Technology*, Transactions of the ASME, vol. 123, no. 2–4, (2001): pp. 270–276.
6. M. Vielma, S. Atmaca, C. Sarica, and H.-Q. Zhang, "Characterization of Oil/Water Flows in Horizontal Pipes," *SPE Projects, Facilities & Construction*, vol. 3, no. 4, (Dec. 2008): pp. 3133–3143.
7. J. Cai, S. Nestic, C. Li, X. Tang, F. Ayello, C. Ivan, T. Cruz, and J. Al-Khamis, "Experimental studies of water wetting in large-diameter horizontal oil/water -pipe flows," SPE Annual Technical Conference and Exhibition (ATCE ), 2005, pp. 719–731.
8. C. Li, X. Tang, F. Ayello, J. Cai, S. Nestic, C. I. Cruz, and J. Al-Khamis, "Experimental study on water wetting and CO2 corrosion in oil-water two-phase flow," CORROSION/2006, paper no. 06595, (Orlando, FL: NACE, 2006).
9. F. Ayello, C. Li, X. Tang, J. Cai, S. Neic, C. I. Cruz, and J. Al-Khamis, "Determination of phase wetting in oil-water pipe flows," CORROSION/2008, paper no.08566 (New Orleans, LA: NACE, 2008).
10. X. Tang, C. Li, F. Ayello, J. Cai, and S. Nestic, "Effect of Oil Type on Phase Wetting Transition and Corrosion in Oil-Water Flow," CORROSION/ 2007, paper no. 07170, (Nashville, TN: NACE, 2007).
11. A. Valle, "CO2-Corrosion and Water Distribution in Two Phase Flow of Hydrocarbon Liquids and Water," CORROSION/2000, paper no. 00047, (Nashville, TN: NACE, 2000).
12. P. Angeli, G.F. Hewitt, "Flow structure in horizontal oil-water flow," *Int. J. Multiphase Flow*, 26 (2000): pp. 1117-1140.
13. J.O. Hinze, "Fundamentals of the hydrodynamic mechanism of splitting in dispersion processes," *A.I.Ch.E. Journal* (1955): pp. 289-295.
14. X. Tang, S. Richter, S. Nestic, and M. Technology, "An Improved Model for Water Wetting Prediction in Oil-Water Two-Phase Flow," CORROSION/2013, paper no.2393 (Orlando, FL: NACE, 2013).
15. D. Barnea, O. Shoham, Y. Taitel, "Transition from annular-flow and from dispersed bubble flow – unified models for the whole range of pipe inclinations," *Int. J. Multiphase Flow*, vol. 12, no.5, (1986): pp. 733-744.
16. N. Brauner, "The prediction of dispersed flows boundaries in liquid-liquid and gas-liquid system," *Int. J. Multiphase Flow*, vol. 27, no.5, (1986), 885-910.